PHYSICAL REVIEW B VOLUME 25, NUMBER 4 15 FEBRUARY 1982

Photoinduced midgap absorption in tetrahedrally bonded amorphous semiconductors

P. O'Connor* and J. Tauc
Department of Physics and Division of Engineering, Brown University, Providence, Rhode Island 02912
(Received 27 April 1981)

Transient photoinduced optical absorption (PA) was used to study the transport, trapping, and recombination of excess electrons and holes in hydrogenated amorphous semiconductors with tetrahedral bonding. The materials studied were *a*-Si:H, *a*-Ge:H, *a*-GaAs:H, and the binary alloy systems *a*-Si_xGe_{1-x}:H and *a*-Si_yC_{1-y}:H prepared by sputtering or glow discharge. In materials with optical energy gaps $E_g \gtrsim 1.25$ eV the absorption arises from transitions between carriers trapped at deep-lying defects and the band edge. This mechanism leads to a threshold in the induced absorption spectrum below E_g. In those compounds with $E_g \lesssim 1.25$ eV the PA spectrum consists of a single symmetric band whose shape can be well explained if absorption is due to photon-assisted hopping of small polarons bound to defects with 0.32—0.40-eV binding energy. The transition between these two spectral shapes as composition is varied appears to be discontinuous. Recombination of these excitations is found to follow bimolecular diffusion-limited kinetics that involves dispersive transport. The time-averaged mobility in *a*-Si:H was on the order of 10^{-3} $cm^2/V\,s$ at room temperature and decreased with decreasing temperature as $\exp(T/T_1)$. A model for this unusual temperature dependence is proposed.

I. INTRODUCTION

The properties of amorphous tetrahedrally bonded semiconductors under illumination have recently been studied by various techniques including photoconductivity,[1,2] photoluminescence,[3] and optically induced paramagnetic resonance.[4,5] The results showed important qualitative similarities to another class of amorphous semiconductors, the chalcogenide-based glasses and amorphous arsenic.[6] The electronic excitations in amorphous semiconductors differ from those in their crystalline counterparts through the presence of a relatively high density of localized states, which may be populated by photoexcited carriers, and where electron-electron and electron-phonon interactions may be enhanced. In the tetrahedrally bonded materials there is a poorer understanding of these states in terms of atomic structure and chemical bonding, particularly regarding the nature of states which may be characterized as structural defects than in the chalcogenide glasses. In both classes of materials, the details of the dynamical processes involving optical and phonon-coupled transitions to and from these states (electron and hole transport, thermalization, and recombination) are not well known.

Investigation of the tetrahedral materials has received additional impetus from the technological potential of hydrogenated amorphous silicon (*a*-Si:H). Most proposed applications for *a*-Si:H are based on its optoelectric (photovoltaic and photoconductive) properties: a better understanding of the photoexcited state is important for the development of these devices.

This paper presents new results on photoinduced optical absorption (PA) below the absorption edge in hydrogenated amorphous tetrahedrally bonded semiconductors which was reported previously.[7—11] The spectrum of the induced absorption is entirely unlike that of photoexcited free carriers in crystalline Si.[12] In some of the materials studied, the induced absorption mechanism appears to be associated with defect states in the gap in a similar way as proposed for the interpretation of the PA band and electron spin resonance (ESR) in chalcogenide glasses[13]; other studied materials have PA spectra which indicate that photoexcited carriers may form small polarons.

The recombination kinetics of electrons and holes has also been studied with this technique. Indirect information about the mobility of the

recombining nonequilibrium electrons can be obtained which shows the influence of localized states on transport in *a*-Si:H and related materials.

Section II presents a description of the experimental procedures. In Sec. III the method of data analysis is discussed. The experimental results appear in Sec. IV and are followed in Sec. V by a general discussion and interpretation of the PA mechanism and of the recombination kinetics. A brief summary and conclusion appear in Sec. VI.

II. EXPERIMENTAL

A. Samples

The experiments were performed on films of various compositions prepared at different laboratories by the sputtering and glow-discharge methods. The composition, preparation technique, energy gap, thickness, and substrate for all samples are given in Table I. The main group of samples were $1-3$-μm thick glow-discharge Si and Ge, and binary alloys of Si with Ge and C whose compositions were determined after deposition by microprobe. We also used glow-discharge *a*-Si:H samples doped *n* and *p* type by the addition of 1 vol % PH_3 or B_2H_5, respectively, in the discharge plasma. The sputtered samples included both hydrogenated (H_2 partial pressure was 8×10^{-4} Torr) and nonhydrogenated *a*-Si and hydrogenated *a*-GaAs. One *a*-Si:H sample (no. 11) was a 14-μm thick film on an etched *a*-Si substrate; this arrangement minimizes thin-film interference effects because of the reduced infrared reflectivity of the sample-substrate interface. All other sputtered samples were $\simeq$1-μm thick and on glass substrates.

Whenever possible, samples were mounted with the substrate side facing the laser. Since the samples are optically thick at the laser wavelength,

TABLE I. Composition, preparation technique, energy gap, thickness, and substrate for all samples. (NA denotes not available.)

Sample	Composition	Preparation method[a]	Optical energy[b] gap	Substrate	Film thickness
1[c]	Si:H	GD	1.65 eV	glass	NA
2	$Si_{0.93}Ge_{0.07}$:H	GD	1.60	glass	1.2 μm
3	$Si_{0.85}Ge_{0.15}$:H	GD	1.55	glass	NA
4	$Si_{0.80}Ge_{0.20}$:H	GD	1.51	glass	1.4
5	$Si_{0.59}Ge_{0.41}$:H	GD	1.36	glass	NA
6	$Si_{0.59}Ge_{0.41}$:H	GD	1.36	glass	1.8
7	$Si_{0.44}Ge_{0.56}$:H	GD	1.26	glass	1.1
8	$Si_{0.35}Ge_{0.65}$:H	GD	1.20	glass	2.6
9	$Si_{0.17}Ge_{0.83}$:H	GD	1.07	glass	0.9
10	Ge:H	GD	0.95	glass	NA
11[d]	Si:H	SP	1.65	*c*-Si	14
12	Si:H	SP	1.65	glass	NA
13	Si:H	SP	1.65	glass	1.09
14	Si	SP		glass	NA
15	Ge:H	SP		Al_2O_3	10
16[e]	Si:H	GD	1.65	Al_2O_3	NA
17[c]	$Si_{0.73}C_{0.27}$:H	GD	1.96	glass	NA
18[d]	GaAs:H	SP	1.26	glass	NA
19[f]	Si:P:H	GD		glass	NA
20	Si:B:H	GD		glass	NA

[a]GD=rf glow-discharge decomposition of $Si:H_4$ in Ar on heated substrate; SP=sputtering in Ar or Ar-H_2 atmosphere, heated substrate.
[b]Defined as intercept of $(\alpha\hbar\omega)^{1/2}$ vs $\hbar\omega$.
[c]Source: IBM San Jose (Guarnieri and Wieder).
[d]Source: Harvard University (Paul and Paesler).
[e]Source: IBM Yorktown Heights (Brodsky).
[f]Source: Xerox Palo Alto (Street and Knights).

pump absorption took place near the sample-substrate interface.

B. Experimental apparatus for steady-state PA

An apparatus which was designed and constructed to measure laser-induced transmission modulation with spectral resolution over the range of transparency of the samples, roughly 0.2—1.8 eV in probe photon energy is shown in Fig. 1. The excitation source (pump) was a 2-W Ar^+ laser. An argon-pumped Rhodamine 6G dye laser was also used in some experiments. The laser was mechanically interrupted by a chopper whose frequency was derived from a lock-in reference oscillator. Residual thermal ir in the pump was filtered out. Typically the laser power absorbed by the sample was about 30 mW. The illuminated area was 3.5×10^{-2} cm^2, hence the absorbed flux was $\simeq2.0\times10^{18}$ photons/cm^{2}s at $h\nu=2.41$ eV. Calibrated neutral-density filters were used to vary the incident intensity by factors from 0.7 to 0.01.

The ir probe system consisted of a source, toroidal focusing and collecting mirrors, and 0.25-m monochromator and detector. For probe wavelengths shorter than 2.5 μm, a 650-W tungsten lamp was used with a room-temperature PbS photoconductor detector. The source was filtered to include only wavelengths to which the sample is normally transparent. At longer wavelengths we used an Opperman source and liquid-nitrogen-cooled PbSe photoconductor. The monochromator was equipped with a variable-rate scanning drive, appropriate gratings (148, 295, 590, and 1180 lines/mm), and order-sorting filters were used to cover the required wavelength range. The probe beam power was adjusted so that the transmitted intensity never exceeded the limits of linear response of the detectors. Samples were mounted on a liquid-nitrogen or liquid-helium coldfinger in an optical transmission Dewar and positioned at the central focus of the probe optical system. The ir spot was adjusted to be completely within the region of the sample illuminated by the pump. Sample temperature could be varied from about 10 to 315 K.

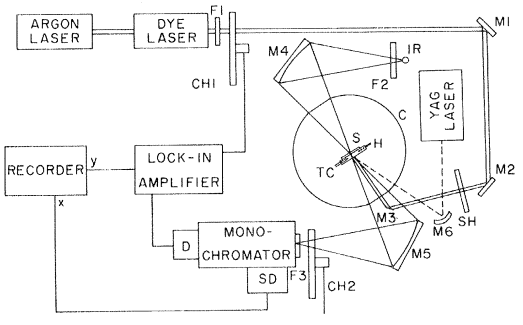

FIG. 1. Experimental arrangement for steady-state induced absorption CH1, 2 choppers; F1 ir suppressing filter; F2 long-wavelength pass filters; F3 order-sorter filter; M1—M5 mirrors; ir tungsten or Opperman ir source; C cryostat; TC thermocouple; H heater; S sample; SH laser shutter; SD scanning drive; D detector.

C. Steady-state PA measurements

Steady-state PA experiments required the measurement of the fractional transmission modulation. $\Delta T/T$, as a function of sample composition, temperature, laser wavelength and intensity, and probe wavelength. Determination of the ratio $\Delta T/T$ was done by first measuring the transmission T with the laser off. The chopped laser beam was then allowed to illuminate the sample. The lock-in signal was then proportional to the synchronous component of the transmission modulation ΔT. Different probe and pump beam choppers were used; both were run at 160 Hz and a correction was made for the slight variation of the lock-in response to the waveforms produced by the different blade geometries.

Under certain conditions the laser excited photoluminescence (PL) from the sample which was inevitably collected, analyzed, and detected along with the transmission modulation signal. Luminescence bands in a-Si_xGe_{1-x}:H occur in the region from 0.7 to 1.5 eV. Since this spectral region overlaps the PA band, filters cannot be used to prevent unwanted PL from reaching the detector. The PL signal is also synchronous with the pump but is 180° out of phase with the transmission modulation caused by induced absorption, hence the two effects tend to mutually cancel. To compensate for this, the PL intensity was separately measured by blocking the probe beam, while allowing the laser to excite the sample and recording the lock-in response. The true $\Delta T/T$ is then the difference of the measured ΔT and PL signals, divided by T. In the worst case the PL signal had a magnitude comparable to ΔT.

Most data taking was done by repeating these two (or three) measurements of T and ΔT (and PL intensity) point by point as some parameter was

varied. However, for measuring the spectrum of $\Delta T/T$ it was necessary to use a different procedure to allow a continuous scan of probe wavelength. This was done by making separate chart recordings of T, ΔT, and PL intensity versus probe wavelength, digitizing the three curves, and computing the true $\Delta T/T$ at closely spaced discrete points. A sampling interval of 0.003 eV was chosen; this is below the resolution limit of the experiment to ensure no loss of information. Typically data was taken in three or four overlapping probe wavelength ranges; $\Delta T/T$ was plotted and adjusted to coincide in the overlap region. The limiting sensitivity of the experiment was $\Delta T/T = 5\times 10^{-6}$, determined by detector dark noise and the constraint of staying in the linear-response region of the detectors.

The temporal response of PA to excitation by 200-ns pulses at 5700 Å was also measured. This work has been presented in a previous publication.[9]

III. ANALYSIS

The transmission modulation spectrum of a thin film produced by small changes $(\Delta\alpha,\Delta n)$ in its optical absorption coefficient and refractive index is not a simple function of frequency because of interference effects. In this section a straightforward averaging procedure is derived which can eliminate these effects and allow the spectrum of induced absorption to be determined from $\Delta T/T$ under certain conditions. In addition, we discuss ways to distinguish refractive-index changes from induced absorption, and the effects of temporal and spatial variations of $\Delta\alpha$ and Δn on the transmission modulation. Finally, changes in the transmission due to thermal modulation of the sample are considered.

A. Thin-film interference effects

Interference effects in modulation spectroscopy of thin films have been treated by Subashiev[14] for the case when the absorption α and refractive index n are uniformly perturbed across the film thickness. Under our actual experimental conditions the optical constants are perturbed only in a thin layer within one laser light absorption depth (α_L^{-1}) of the film front surface. Taking the optical properties of the transparent substrate to be equal to those of the vacuum, the unmodulated transmission coefficient has the familar wavelength-dependent thin-film form:

$$T=\frac{(1-R)^2e^{-\alpha d}}{1+R^2e^{-2\alpha d}-2R\cos 2\delta}\ . \tag{1}$$

If we consider the effects of a small modulation of α and n within the pumped layer on the absorption, front-surface reflectivity, and phase shift of the film to first order only, then the fractional transmission modulation can be written[11]

$$\frac{\Delta T}{T}=f_1(\Delta\alpha/\alpha_L)+f_2\Delta n\ , \tag{2}$$

where

$$f_1=\frac{T(R^2e^{-\alpha d}-e^{\alpha d})}{(1-R)^2}\ , \tag{3a}$$

$$f_2=\frac{-4TR}{(n^2-1)(1-R)^3}e^{\alpha d}+Re^{-\alpha d} -(1+R)\cos 2\delta +2\pi(n^2-1)(1-R)\frac{\sin 2\delta}{\lambda\alpha_L}\ . \tag{3b}$$

In the above formulas n and α are the unmodulated refractive index and absorption coefficient of the sample, R is its Fresnel reflectivity, λ is the probe wavelength, and $\delta=2\pi nd/\lambda$ is the optical phase shift per pass. The expressions (1), (3a), and (3b) are valid for probe light whose longitudinal coherence length greatly exceeds the film thickness d.

The coefficients f_1,f_2 are plotted in Fig. 2 as a function of normalized probe photon energy for two sets of sample parameters. The optical constants α,n are taken as independent of energy to show the interference structure. Note that f_1 is a negative definite function while f_2, the coefficient of Δn, exhibits oscillatory sign changes. The interference pattern of f_1 is a sign-reversed replica of T (same peak positions and fringe contrast) but the oscillations in f_2 increase in amplitude with increased energy. These qualitative characteristics help to distinguish whether induced absorption or induced index changes make the dominant contribution to $\Delta T/T$.

In the modulation spectroscopy experiment, physically interesting information about the material is contained in the spectrum of $\Delta\alpha(h\nu)$ and $\Delta n(h\nu)$, but as seen in Fig. 2 interference effects can easily obscure this. To minimize the quasiperiodic fringe pattern associated with the coefficients f_1 and f_2

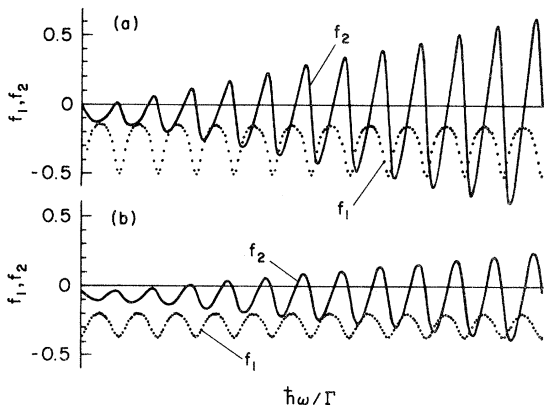

FIG. 2. Coefficients of $\Delta T/T$, f_1 (broken line) and f_2 (solid lines), vs probe photon energy for $R=0.3$, $n=3.5$, $d=10^{-4}$ cm, $\alpha_L=10^5$ cm^{-1}. In (a) $e^{-\alpha d}=1$; in (b) $e^{-\alpha d}=0.5$.

it is desirable to work with the cycle-averaged relative transmission modulation, defined as

$$\frac{\overline{\Delta T}}{T}=\frac{1}{F}\int_{h\nu-F/2}^{h\nu+F/2}\frac{\Delta T}{T}(h\nu')\,d(h\nu')\ . \tag{4}$$

When α and n vary slowly on the scale of the fringe period $F=hc/2nd$ then this quantity is given by

$$\frac{\overline{\Delta T}}{T}=\bar{f}_1\Delta\alpha/\alpha_L+\bar{f}_2\Delta n\ . \tag{5}$$

Since the coefficient f_1 is strictly periodic, it averages to a constant. But f_2 contains a term proprotional to $(\sin 2\delta)/\lambda$; this gives rise to a small residual oscillation in $\bar{f}_2$. It can be shown[11] analytically that

$$\bar{f}_1\equiv -1\ , \tag{6a}$$

$$\bar{f}_2=\frac{A}{2}\sum_{n=0}^{\infty}B^n\left[\frac{(-1)^n}{n+1}\cos^{n+1}2\delta+K_n\right]\ , \tag{6b}$$

where in (6b)

$$A=\frac{(1-R)^2e^{-\alpha d}}{1+R^2e^{-\alpha d}},\quad B=\frac{2Re^{-\alpha d}}{1+R^2e^{-\alpha d}} \tag{7}$$

and

$$K_n=\begin{cases}\dfrac{1}{(n+1)2^{n+1}}\left[\begin{matrix}n+1\\ \frac{1}{2}(n+1)\end{matrix}\right], & n \text{ odd}\\ 0, & n \text{ even}\ .\end{cases} \tag{8}$$

For typical sample parameters ($R=0.3$, $\alpha d=0$) f_2 can be approximated by

$$f_2=-0.17+(4\times10^{-3})\cos^2 2\delta\ . \tag{9}$$

Hence the relative contribution to $\Delta T/T$ from index modulation is small and the presence or absence of sign changes in the nonaveraged $\Delta T/T$ can be used to judge when it exists.

B. Nonuniform optical constants

In Sec. III A it was assumed that perturbation of the optical constants occurs uniformly in a thin layer within α_L^{-1} from the front surface. In the more realistic case where $\Delta\alpha$ and Δn have continuously varying profiles $\Delta\alpha(z)$, $\Delta n(z)$ through the film, the transmission modulation due to induced absorption in a film of thickness d is, neglecting interference effects:

$$\frac{\Delta T}{T}=\exp\left[-\int_0^d\Delta\alpha(z)dz\right]-1$$
$$\simeq-\int_0^d\Delta\alpha(z)dz\ . \tag{10}$$

If the film has refractive index n and $\Delta n<<n$ everywhere, then it can also be shown[11] that to lowest order in Δn the transmission modulation becomes

$$\frac{\Delta T}{T}=\frac{-4n}{d(n^2+1)}\int_0^d\Delta n(z)dz\ . \tag{11}$$

Hence, for the bulk samples $\Delta T/T$ depends to first order on the integrated (or total) induced absorption or index change and is insensitive to their profiles. The results of Sec. III A for the steady-state cycle-averaged transmission modulation can therefore be taken over to the case of nonuniform perturbation if the quantities $\Delta\alpha/\alpha_L$ and Δn are replaced by suitable average values over the region of strong laser absorption.

For the time-resolved induced absorption $\Delta T/T$ is given by

$$\frac{\Delta T}{T}(t)\simeq-\int_0^d\Delta\alpha(z,t)dz\ . \tag{12}$$

When the space and time dependence of the induced absorption are coupled, then the time decay of $\Delta T/T$ cannot be easily interpreted unless the form of $\Delta\alpha(z,t)$ is already known.

C. Bolometric effects

The photons of the periodically interrupted pump beam are strongly absorbed by the sample,

creating electron-hole pairs. Since the quantum efficiency for radiative recombination is low in most samples, the energy deposited by the laser is eventually dissipated as heat to the lattice. The heat generated raises the sample temperature from T to $T+\Theta$. The magnitude of the maximum temperature modulation (ac component of Θ) and of the steady-state heating caused by the laser (dc component) can be estimated by using an electrical analog to the thermal circuit consisting of film, substrate, and mount with input heat generation from laser absorption.[15] We find in the worst case a thermal modulation of 0.3 K superimposed on an 8-K steady heating.

There are four ways in which sample heating can effect the optical properties of the sample in the infrared. The number of carriers thermally generated by a temperature rise of 0.3 K is negligible in comparison to the optically generated carrier density. The film thickness change from thermal expansion is also much too small to produce an observable phase shift of the interference pattern.

Significant thermal effects can result from the temperature dependence of the fundamental absorption edge and its associated refractive-index dispersion. For small temperature modulation $\Delta\Theta$, the optical constants will be modified by the amounts

$$\Delta\alpha=\frac{d\alpha}{d\Theta}\Delta\Theta\ , \tag{13a}$$

$$\Delta n=\frac{dn}{d\Theta}\Delta\Theta\ . \tag{13b}$$

Using a simplified formula for $\Delta T/T$ which neglects interference effects and taking the sensitivity of the experiment to be $\Delta T/T\geq 10^{-5}$, we can determine limiting values of the coefficients which will produce observable transmission modulation for a $\Delta\Theta$ of 0.3 K:

$$\frac{1}{\alpha}\frac{d\alpha}{d\Theta}\geq 3\times 10^{-1}\ \mathrm{K}^{-1}\ , \tag{14a}$$

$$\frac{dn}{d\Theta}\geq 2.8\times 10^{-4}\ \mathrm{K}^{-1}\ . \tag{14b}$$

The coefficient in (14a) can be estimated from published data[16] by assuming a rigid shift of the absorption edge with temperature. We find $d\alpha/d\Theta=(6.4\times 10^{-4}\ \mathrm{K}^{-1})\alpha$ in hydrogenated a-Si, and roughly half that value in a-Si without hydrogen. The limiting value given in (14a) is reached in a-Si:H when the probe energy exceeds 1.65–1.75 eV, hence thermal modulation of the absorption coefficient of the sample is expected to be insignificant in the wavelength range of our measurements. However, in nonhydrogenated sputtered a-Si, the absorption edge has a long tail extending into the ir. The thermal shift of this edge is estimated to produce an observable $\Delta T/T$ at photon energies equal to or exceeding 0.8 eV, well within the experimental range probed here. Evidence of a thermal effect of this type was, in fact, seen in sample no. 14 (see Sec. IV).

The temperature dependence of the refractive index of glow-discharge deposited a-Si:H has also been reported in the literature.[17] $dn/d\Theta$ reaches the limiting value (14b) at the photon energy of 1.2 eV and increases strongly at higher energies. The refractive-index change also contributes an additional phase shift which results in positive- and negative-going oscillations (of roughly equal amplitude) in $\Delta T/T$ when interference effects are considered (see Sec. III A). The presence of such oscillations is a necessary signature of refractive-index modulation.

IV. RESULTS

A. Spectra

In Figs. 3(a)–3(d) are shown the normalized steady-state induced absorption (PA) spectra for four representative glow-discharge Si-Ge alloys at 80 K. Figure 4 shows the PA spectra of hydrogenated and nonhydrogenated sputtered a-Si, hydrogenated sputtered a-GaAs, and glow discharge a-$Si_{0.73}C_{0.27}$:H. For those samples which exhibit interference effects, the numerically averaged quantity $\overline{\Delta T/T}$ discussed in Sec. III is also shown (smooth lines). In Fig. 3(a) there is a sharp increase in $|\Delta T/T|$ above 1.7 eV; this is due to a thermally induced downward shift of the fundamental absorption edge as discussed in Sec. III C. It is also likely that the induced absorption in nonhydrogenated amorphous Si [Fig. 4(b)] is due solely to a thermal effect for the reasons discussed in Sec. III C.

It will be generally assumed in the rest of this section that with the exceptions noted above, the cycle-averaged quantity $\overline{\Delta T/T}$ is proportional to the spectrum of the induced absorption coefficient $\Delta\alpha(\hbar\omega)$ for all samples; any weak structure in the spectra on the scale of interference fringe spacing is considered unresolvable.

In order to more clearly exhibit the shapes of the induced absorption bands, the spectra of Figs. 3 and 4 have been plotted on normalized vertical

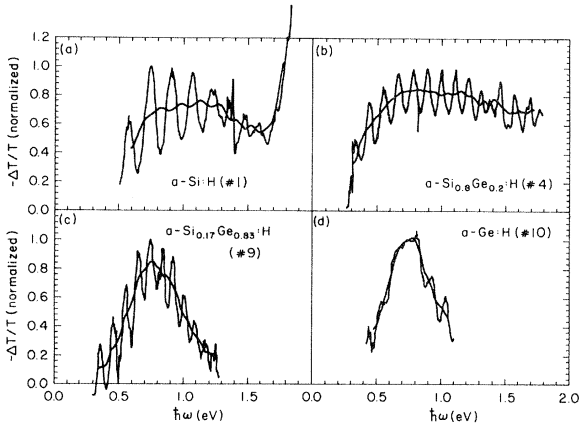

FIG. 3. Normalized induced absorption spectra for four glow-discharge a-Si_xGe_{1-x}:H samples at 80 K. Numerically averaged spectra for those samples exhibiting interference fringes are also shown (smooth lines).

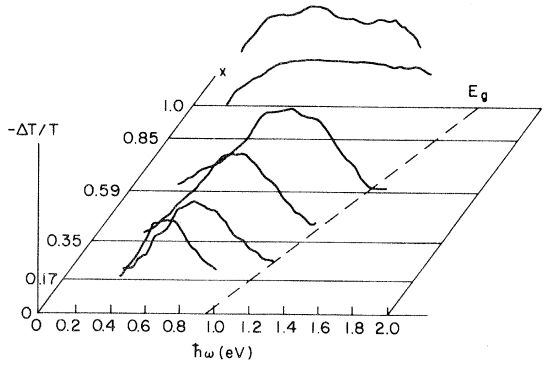

FIG. 5. Induced absorption in the binary alloy system a-Si_xGe_{1-x}:H as a function of probe photon energy and alloy composition x. Broken line: optical energy gap E_g as a function of composition.

scales. However, the magnitude of $|\Delta T/T|$ at the peak is not strongly composition dependent. In addition, care was not taken to make precise measurement of the absolute $|\Delta T/T|$ because of the difficulty of achieving accurately reproducible optical alignment and because of the observed variations in the strength of the effect from spot to spot on the sample. The magnitude of the peak $|\Delta T/T|$ at 80 K in the samples of Figs. 3 and 4 is between 8×10^{-5} and 7×10^{-4}.

Figure 5 shows the normalized and averaged induced absorption spectra of several samples in the a-Si_xGe_{1-x}:H binary system on the photon energy-alloy composition plane (samples nos. 1, 3, 6, 8, and 9). Also shown (dashed line) is the optical energy gap E_g, defined as the intercept of the straight portion of the $(\alpha\hbar\omega)^{1/2}$ vs $\hbar\omega$ plot, where α is the absorption coefficient. For amorphous Ge, a single symmetric peak at around 0.75 eV is seen; as the fraction of silicon in the alloy increases, the band broadens and shifts to higher energies, losing the roughly Gaussian shape, and becoming asymmetric in Si-rich samples. Outside the Si-Ge binary alloys, we find a rough correlation of the half-width of the PA spectrum with band gap. This is shown in Fig. 6, where the abscissa is the optical gap E_g defined above. The

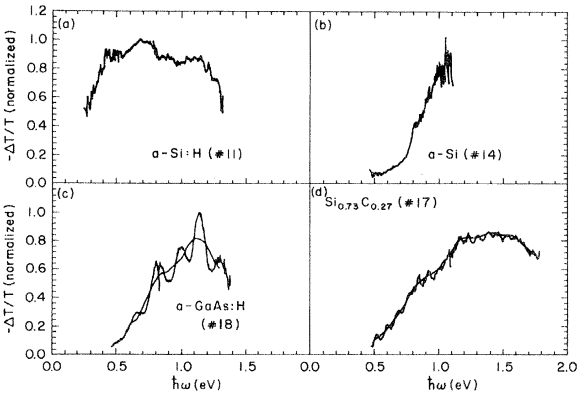

FIG. 4. Normalized 80 K induced absorption spectra of (a) sputtered a-Si:H, (b) nonhydrogenated sputtered a-Si, (c) sputtered a-GaAs:H, and (d) glow-discharge a-$Si_{0.73}C_{0.27}$:H.

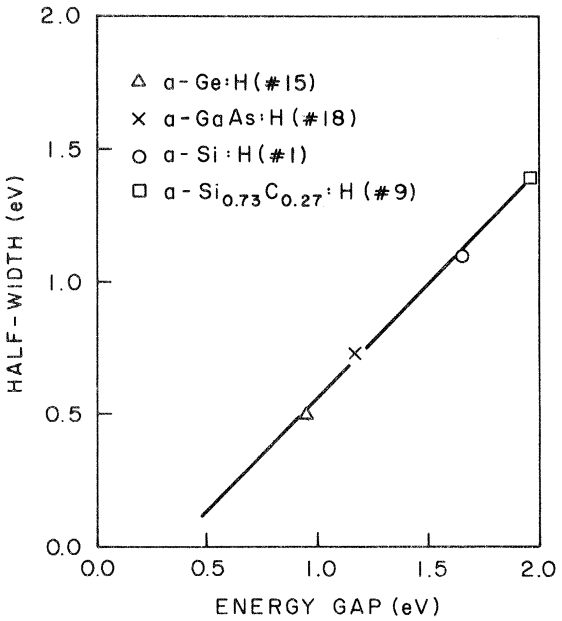

FIG. 6. Induced absorption band FWHM vs optical energy gap for glow-discharge a-Ge:H, a-GaAs-H, a-Si:H, and a-$Si_{0.73}C_{0.27}$:H.

values of E_g were taken from the literature for *a*-Ge:H, *a*-Si:H,[18] and *a*-GaAs:H,[19] and $E_g = 1.96$ eV was found for the $Si_{0.73}C_{0.27}$ alloy from transmission measurements.

The temperature dependence of the spectra of several samples from 80 to 300 K is shown in Fig. 7. The shape of the single symmetric peak in a Ge-rich alloy is seen to be nearly independent of temperature, while the broad spectrum of *a*-Si:H at 80 K narrows appreciably with increasing temperature. The numbers in parentheses are the normalization factors for each curve; note that in both these samples (a) and (b) the PA decreases strongly with increasing temperature. In Figs. 7(c) and 7(d) the spectra of the two doped samples are shown; the temperature dependence of the spectral shapes is relatively weak. In particular, there is no strong narrowing seen as in *a*-Si:H.

B. Intensity dependence and excitation spectra

When illuminated with laser (pump) light of 2.41-eV photon energy, most samples showed a power-law variation of PA with pump intensity I_L ($\Delta T/T \propto I_L^s$), with $0.50 \leq s \leq 0.65$. This behavior was found at all temperatures and probe wavelengths, with the exception of a Ge-rich alloy which had $0.31 < s < 0.37$. However, the intensity dependence in this sample could also be fit to $\Delta T/T \propto \log I_L$, which is the form expected if the density of absorbing centers saturates.

Similar square-root dependence ($\Delta T/T \sim I_L^{0.5}$) was generally observed when the samples were illuminated with a tunable dye laser with photon energies in the range 2.0—2.20 eV. However, in the sample with the highest energy band gap (*a*-$Si_{0.73}C_{0.27}$:H, no. 17) the pump wavelength and intensity dependence were interrelated. This is shown in Fig. 8 where we plot the log of $\Delta T/T$ (at 0.8-eV probe) vs I_L for various wavelengths of the dye laser pump. At these wavelengths the absorption coefficient of the sample is between 2×10^3 and 1.5×10^4 cm^{-1}. For low and moderate intensities, induced absorption is a linear function of I_L, except at the highest pump photon energy ($\hbar\omega_L = 1.275$ eV) where s decreases to 0.86. With argon laser excitation ($2.4 < \hbar\omega_L < 2.75$ eV), however, we observed $s = 0.5-0.6$ in this sample. The absorption coefficient exceeds 5×10^{-4} cm^{-1} at these wavelengths. Thus a continuous change from linear to square-root dependence of $\Delta T/T$ on pump intensity occurs as $\hbar\omega_L$ sweeps through the absorption edge.

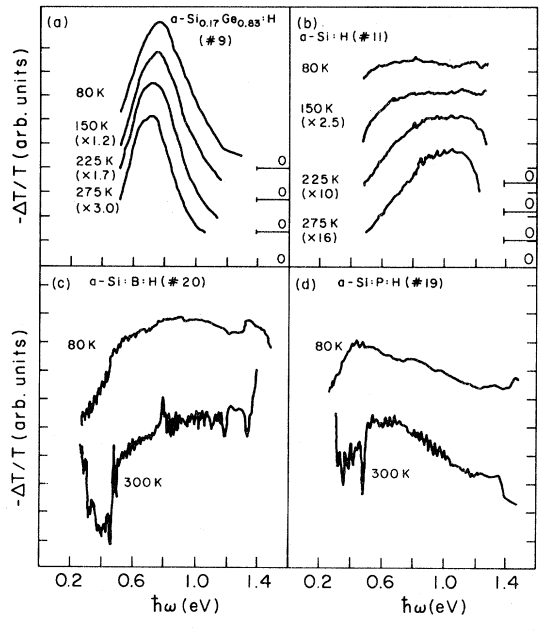

FIG. 7. Normalized induced absorption spectra at various temperatures for (a) glow-discharge *a*-$Si_{0.17}$ $Ge_{0.83}$:H, (b) sputtered *a*-Si:H, (c) glow-discharge *a*-Si:B,H, and (d) glow-discharge *a*-Si:P:H.

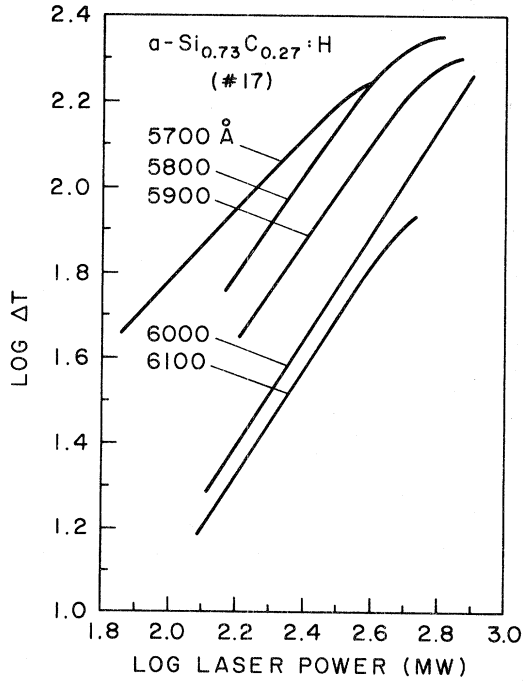

FIG. 8. Pump intensity dependence of PA in *a*-$Si_{0.72}C_{0.27}$:H at several excitation wavelengths.

We can define an efficiency η as

$$\eta=\frac{(\Delta T/T)\hbar\omega_L}{I_L[1-T/(1-R)^2]}\ , \tag{15}$$

which represents the induced steady-state transmission modulation per absorbed photon per second. This quantity for the a-$Si_{0.73}C_{0.27}$:H alloy is roughly constant in the absorption-edge region, but an anomalously high value occurs at the lowest excitation photon energy ($\hbar\omega_L=2.00$ eV); this measurement was reproduced several times and seems to be outside the bounds of experimental error.

Figure 9 is a plot of the PA quantum efficiency η at 80 K as a function of photon energy in the high-absorption region ($\hbar\omega_L>2.4$ eV) for three binary alloys of group IV elements. The laser light absorption coefficient α_L exceeds 5×10^4 cm^{-1} for all samples in this region and is an increasing function of energy. All samples show a weak downward trend in $\eta(\hbar\omega_L)$ above 2.41 eV, indicative of a stronger decrease of the true quantum efficiency per absorbed photon. Interface effects, which become more pronounced as the laser absorption depth decreases, may account for the observed falloff of η at high energies.

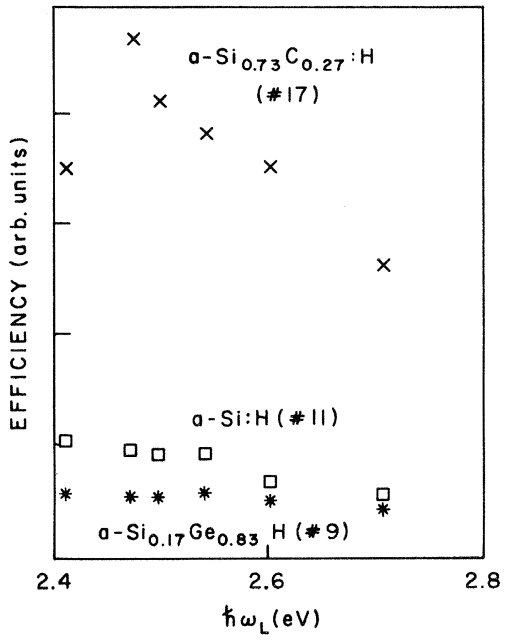

FIG. 9. Efficiency of PA per absorbed photon vs pump photon energy $\hbar\omega_L$ for a-Si:H, a-$Si_{0.17}Ge_{0.83}$:H, and a-$Si_{0.73}C_{0.27}$:H excited by argon laser.

C. Temperature dependence

Steady-state induced absorption was strongly quenched with increasing temperature in all samples, and in many cases the quenching exhibited a well-defined thermal activation energy at high temperatures, i.e.,

$$-\Delta T/T\propto\exp(\Delta E/kT)\ ,$$

with ΔE in the range 0.07–0.12 eV. Below about 200 K the induced absorption gradually saturates. The same behavior was obtained for these samples at various pump levels; this implies that the leveling off of PA at low temperatures is not due to saturating a fixed number of absorbing centers.

It is more meaningful to discuss the temperature dependence of the steady-state PA in terms of the bimolecular recombination coefficient b which controls the density of absorbing centers. Neglecting the effects of a refractive-index modulation (justified from the absence of alternating-sign oscillations in $\Delta T/T$ vs $h\nu$), the spectrally integrated transmission modulation can be written as the integral over the inhomogeneous spatial carrier profile $n(z)$:

$$\frac{-\Delta T}{T}=\int_0^d\Delta\alpha_{\rm tot}(z)dz=\sigma\int_0^d n(z)dz\ , \tag{16}$$

where z is the distance from the sample front surface, d is the sample thickness, σ is the induced absorption cross section, and n refers to the density of induced absorbing centers. From the square-root dependence of PA on laser intensity we assume that the PA excitation recombines by a bulk bimolecular mechanism. Then the density $n(z)$ is the steady-state solution of the nonlinear diffusion equation

$$\frac{\partial n}{\partial t}=D\frac{\partial^2 n}{\partial z^2}+G(z)-bn^2=0\ , \tag{17}$$

where D is the diffusion coefficient, b is the bimolecular rate coefficient, and the optical generation rate $G(z)$ is given by

$$G(z)=\alpha_L F(1-R)\exp(-\alpha_L z)\ , \tag{18}$$

where F is the incident photon flux, and α_L and R are the absorption coefficient and reflectivity of the sample at the pump-wavelength. If the diffusion coefficient of the PA centers is sufficiently small, then the first term on the right of Eq. (17) can be neglected, giving

$$n(z) = |G(z)/b|^{1/2} . \quad (19)$$

Equations (18) and (19) are substituted into Eq. (16) to give

$$\frac{-\Delta T}{T} = 2\sigma \left[\frac{F(1-R)}{\alpha_L b} \right]^{1/2} , \quad (20)$$

since $\alpha_L d >> 1$. Solving (20) for the bimolecular coefficient, we obtain finally

$$b = \frac{4\sigma^2 F(1-R)}{(-\Delta T/T)^2 \alpha_L} . \quad (21)$$

Figure 10 shows $b(T)$ calculated from (21) for three representative samples. To apply formula (21), we use $\sigma = 10^{-16}$ cm^2 and α_L for a-Si:H at 2.41 eV was taken from the literature[16] and corrected for its temperature dependence. In Fig. 10 the results for the two sputtered a-Si samples show good agreement for the activation energy of the recombination rate coefficient at high temperatures ($\Delta E_b \simeq 0.12$ eV) and the temperature at which saturation sets in ($T_s \simeq 160$ K). In the Ge-rich alloy sample the thermal activation was stronger and saturation set in at a higher temperature.

The temperature dependence in the whole temperature range of the PA in a-Si:H is well described by the functional form $(-\Delta T/T) \sim \exp(-T/T_2)$, where T_2 is a constant. This behavior is illustrated

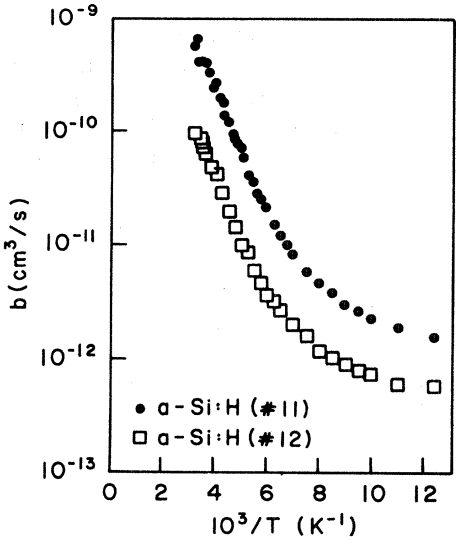

FIG. 10 Temperature dependence of the bimolecular recombination coefficient to two sputtered a-Si:H samples. Spectrally integrated PA band was measured.

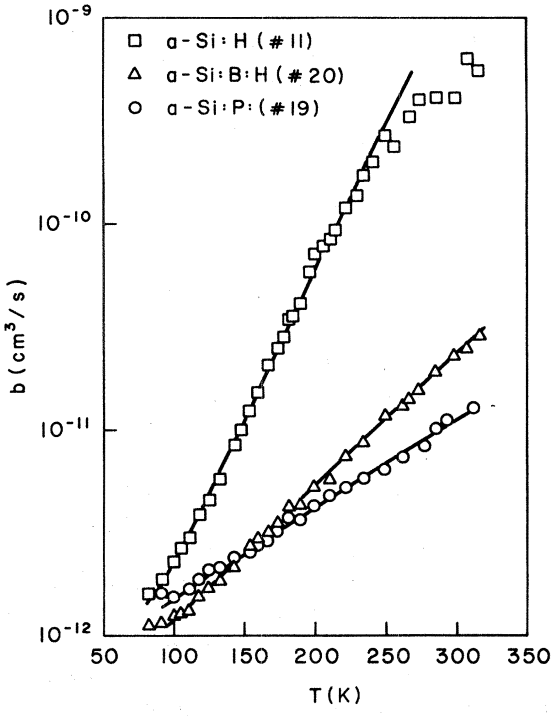

FIG. 11 Temperature dependence of the bimolecular recombination coefficient in doped and undoped a-Si:H. Coefficient b is porportional to electron mobility.

in Fig. 11, where $\ln b$ is plotted as a function of T (linear scale). It is found that $b \sim \exp(T/T_1)$. Since $(-\Delta T/T) \sim b^{-1/2}$ from Eq. (19) above, the slope $T_2 = 2T_1$. This unusual temperature dependence will be discussed further in Sec. V.

It should be noted that the value of b calculated from (21) is strongly dependent on the absorption cross section per carrier σ ($\equiv \Delta\alpha/N$) which is not accurately known for the PA transition. We obtained an estimate of σ from the measured $\Delta\alpha$ and an estimate of N.

An attempt was made to bleach the induced absorption in sputtered a-Si:H sample no. 12 by using intense light at $\hbar\omega = 1.1$ eV from a 2-W YAG (yttrium aluminum garnet) laser. From Fig. 3(a), it can be seen that this light lies in the upper portion of the PA band. No observable bleaching above the limit of experimental error ($\sim 5\%$) was seen. However, this may have been due to the relatively low absorption in the PA band (≤ 20 cm^{-1}). If the rate of optical quenching is proportional to the volume rate of photon absorption in the PA band, then the relative decrease of PA should be proportional to the ratio of the quenching rate Q to the generation rate G:

$$\frac{\delta(\Delta T/T)}{\Delta T/T}=\frac{Q}{G}=\frac{I_{\mathrm{YAG}}\Delta\alpha(1.1\ \mathrm{eV})}{I_{\mathrm{Ar}}\alpha(2.41\ \mathrm{eV})}$$

$$\simeq\frac{2\ \mathrm{W}}{0.03\ \mathrm{W}}\frac{20\ \mathrm{cm}^{-1}}{10^5\ \mathrm{cm}^{-1}}=1.3\%$$

which was unobservable.

V. DISCUSSION

A. Nature of the PA centers in amorphous hydrogenated silicon, silicon-carbon, and Si_xGe_{1-x} with $x>0.6$

In these materials, characterized by band gaps ≥ 1.4 eV, the PA spectra are usually asymmetric bands having a relatively steep rise at low energies and a gradual decline above the peak, which can occur from 0.7 to 1.4 eV. It was shown in a previous publication[10] that this shape is consistent with optical transitions from deep, discrete traps to a band of extended states. To be observed in photoinduced absorption the initial (trap) states for this "photoionization" transition must be between quasi-Fermi-levels E_{tn} and E_{tp} for electrons and holes in gap states. If the matrix element is independent of energy and the continuum has a density of states which increases like $(E-E_c)^{1/2}$ [or $(E_v-E)^{1/2}$ for hole transitions], then the induced absorption coefficient $\Delta\alpha$ has the form[10]

$$\Delta\alpha(\omega)=\frac{\pi\mu ce^2}{2nm^2\omega}N_TN_c[\hbar\omega-(E_c-E_T)]^{1/2}\ , \tag{22}$$

where N_c is the density of states at the band edge E_c. The trap is taken to be a discrete level at E_T described by a density of states

$$g(E)=N_T\delta(E-E_T)\ .$$

To illustrate the fit of Eq. (22) to the data, Fig. 12 shows the smoothed PA spectra of several samples in this group plotted as $(\Delta\alpha\hbar\omega)^2$ vs probe photon energy $\hbar\omega$. The fit is satisfactory over a large energy range, with threshold energies of 0.38 and 0.55 eV for sputtered and glow-discharge a-Si:H, respectively. Figure 13 shows the measured temperature dependence of E_T.

If the distribution of states in the gap is broad rather than discrete, then the induced absorption spectrum due to photoionization of trapped centers is no longer given by (22). Instead, the convolution of the trap-state density in the gap $g_T(E)$ with the band density of states, multiplied by the appropriate combination of occupancy factors, must be used. In general, such a spectrum should have a threshold at $\hbar\omega_T=E_c-E_{tn}$ (for electron transitions) or $E_{tp}-E_v$ (for holes), where E_c and E_v are the conduction- and valence-band edges, respectively. Above this threshold, the broadening of the trap level should cause the PA to increase with energy more rapidly than in Eq. (22). Since the gap states in a-Si:H are undoubtedly broadly distributed, the absence of upward curvature in the data of Fig. 12 indicates that only states near the trap quasi-Fermi-levels are effective as initial states for photoionization.

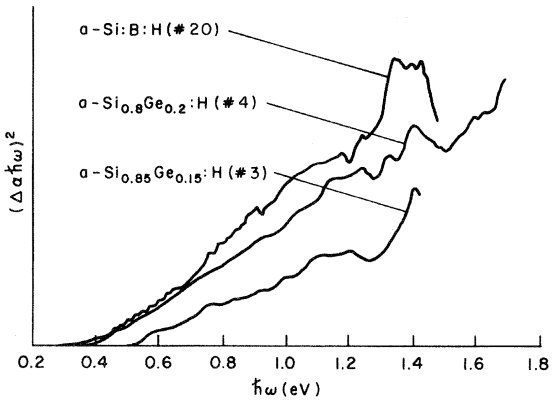

FIG. 12. Induced absorption coefficient plotted as $(\Delta\alpha\hbar\omega)^2$ vs $\hbar\omega$ at 80 K.

The reason for this behavior becomes clear when examined in conjunction with the temperature dependence of the total (spectrally integrated) PA [$\Delta T/T$ from Eq. (21) and Fig. 11]. The total PA is proportional to the total density of trapped car-

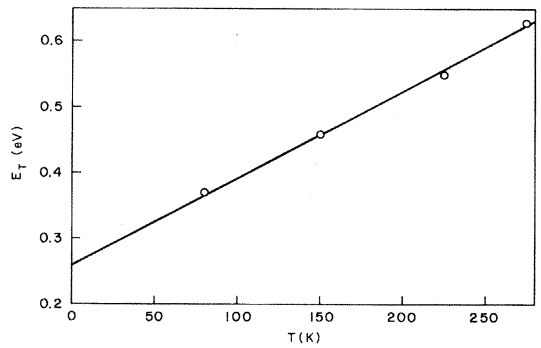

FIG. 13. Temperature dependence of induced absorption threshold $\hbar\omega_T$ in a-Si:H (sample no. 11).

riers, which in quasiequilibrium fully occupy the states between E_F and the quasi-Fermi-levels:

$$p_t = \int_{E_{tp}}^{E_F} g(E)dE \ , \tag{23a}$$

$$n_t = \int_{E_F}^{E_{tn}} g(E)dE \ . \tag{23b}$$

E_{tn} and E_{tp} are functions of temperature because of the temperature dependence of the recombination rate (see Sec. V C below). The inward motion of the quasi-Fermi-levels with increasing temperature is manifested in two ways: by an increase in the PA threshold energy $\hbar\omega_T$ and by a decrease in the total PA proportional to the change in p_t or n_t. For reasons given below, we restrict discussion here to hole transitions. Differentiating (23a) gives

$$g(E) = -\left[\frac{dp_t}{dE_{tp}}\right]_{E_{tp}=E} = \left[\frac{dp_t}{dT}\right] \Big/ \left[\frac{d\hbar\omega}{dT}\right]_{\hbar\omega_T = E - E_v} . \tag{24}$$

The right-hand side of (24) can be evaluated from the data of Figs. 11 and 13 for a sputtered a-Si:H sample no. 11. From the exponential decrease of total PA with equal increments of E_{tp}, we find that the gap density of states in the region from 0.37 to 0.63 eV above the valence-band edge is of the form

$$g(E) = \text{const} \times e^{-E/E_1}$$

with the characteristic width E_1 of the distribution given by

$$E_1 = \left[\frac{d\hbar\omega_T}{dT}\right] \Big/ \left[\frac{-d\ln p_t}{dT}\right]$$

$$= (1.3 \times 10^{-3} \text{ eV/K})\ (62 \text{ K}) = 0.085 \text{ eV} \ .$$

The magnitude of the density of states can also be deduced by relating the integrated induced absorption coefficient $\Delta\alpha$ to the trapped carrier density, using a reasonable value (10^{-16} cm^2) for the absorption cross section per trapped hole. This gives a density of states $g(E_v + 0.37 \text{ eV}) = 7 \times 10^{17}$ cm^{-3}eV^{-1}, falling to 3×10^{16} cm^{-3}eV^{-1} at $E_v + 0.63$ eV. Note that these conclusions are based on an energy-independent matrix element for absorption and that the exponential behavior of $g(E)$ does not necessarily extrapolate to regions of the gap other than the range through which E_{tp} moves in our experiments.

The exponential falloff of the trap-state density towards midgap gives a simple physical explanation for the PA line shape near threshold, which is close to the form expected for discrete, delta-function trap energy. The density of occupied states is the product of $g(E)$ with the nonequilibrium occupancy function which falls off sharply below E_{tp}. Thus the trapped holes have a distribution which is sharply spiked at E_{tp}. This effect was also mentioned in a recent treatment of trap-limited mobility in amorphous semiconductors.[20]

The assumption that PA in these materials is due to photoionization of trapped holes rather than electrons, is supported by several other recent experiments which give evidence for hole-trapping states in a-Si:H in semiquantitative agreement with our results. In particular, the drift mobility of holes is found to be thermally activated with an activation energy of 0.3—0.4 eV.[21] This represents the thermal energy needed to excite a trapped hole to the valence band. In a study of thermally stimulated currents in a-Si:H Schottky solar cell structures, Vieux-Rochaz *et al.*[22] found evidence of 10^{18}-cm^{-3} hole traps at $E_v + 0.13$ eV and no observable electron traps.

Recently infrared quenching of photoconductivity (PC) in high purity a-Si:H has been observed.[23] The PC quenching spectrum is strikingly similar to the induced absorption band reported in this work. The authors of Ref. 23 suggest that the effect is brought about by transition of holes out of trap states into the valence band where they can then be transported to recombination centers. This interpretation is analogous to the classical explanation of optical quenching of PC in crystalline photoconductors.[24]

The equilibrium absorption below the band gap in a-Si:H has been measured[2] by sensitive photoconductivity threshold techniques.[24] The absorption shoulder in region 1.1—1.3 eV of magnitude $\alpha \sim 5 - 50$ cm^{-1} found by Crandall and others[2,25] was interpreted as being due to transitions of electrons from states in the gap around 0.4 eV above the valence band to E_c. If this interpretation is correct, it supports the hypothesis that the PA is due to transitions of trapped holes in the same gap states to the valence-band edge, because the absorption has the same magnitude, and the sum of the equilibrium (1.2 eV) and PA (0.65 eV) threshold energies roughly equals the band gap.

Although photoionization of trapped holes is the

likely mechanism of PA in *a*-Si:H, the results of this work do not rule out other interpretations. In particular, phononless optical charge transfer of electrons was recently observed to give appreciable ir absorption by Hauser *et al.*[26] in sputtered semiconducting Si-Au alloys without hydrogen. This absorption also had an asymmetric spectrum whose shape and peak position strongly resemble the PA bands of Fig. 3. The authors attributed the absorption to hopping of electrons among states near the Fermi level localized at the Au atoms. However, the magnitude of the absorption ($\alpha \sim |g(E_F)|^2$) did not extrapolate to zero at zero Au concentration. In *a*-Si:H, in the dark $g(E_F)$ is too small for these transitions to give any appreciable equilibrium absorption in the ir. In photoexcited *a*-Si:H the occupation of similar states in the gap (near quasi-Fermi levels) by trapped carriers might be expected to lead to observable absorption by the same mechanism. The magnitude of $\Delta\alpha$ is proportional to $|g(E_{tn})|^2$ or $|g(E_{tp})|^2$; comparing our data with that of Ref. 26 we find that a density of $\sim 4\times 10^{19}$ cm^{-3} at the electron or hole trap quasi-fermi level would be required for the observed peak $\Delta\alpha$ of ~ 20 cm^{-1}.

In their recent observation of room-temperature PA in *a*-Si:H, Olivier *et al.*[27] found a spectrum similar to that of Fig. 3 over the restricted spectral range 0.8—1.2 eV with a magnitude and intensity dependence in rough agreement with our results. They also attributed the observed PA to photoionization of trapped holes, but gave no arguments ruling out optical transitions of trapped electrons.

The nature of the states which trap holes and lead to PA in *a*-Si:H is not known. The two simplest point defects in a tetrahedral random network, the dangling bond and vacancy (or vacancy cluster) are each expected to have donorlike and acceptorlike states in the gap. In fact, states having the appropriate spin and change properties are seen in ESR.[4,5] In addition, a third ESR signal at $g=2.011$ is seen under illumination or when the Fermi level is shifted to the lower half of the gap by *p*-type doping.[28] This is apparently due to a more complex defect structure such as a dangling bond dimer, double dangling bond, or a state associated with hydrogen. This donorlike defect, which makes the major contribution to the state density in the lower half of the gap, is the most likely initial state for the proposed PA transition.

Another possibility, namely, that the defect responsible for PA is created by the strongly absorbed pump light, was not investigated. The apparent agreement of the defect energy levels with those found by optical, electrical, and ESR experiments in the dark and the rapid (~ 60 μsec) decay of PA following pulsed excitation at 300 K make it implausible to ascribe the PA effect to photostructural changes. However, evidence has been presented which distinguishes both "native" and photoinduced defects with similar properties in the chalcogenide glasses[29]; this possibility cannot be entirely ruled out in *a*-Si:H.

B. PA centers in germanium, Si_xGe_{1-x} with $x < 1.6$ and GaAs

The group-IV materials in this category have PA spectra which show a symmetric peak at 0.7—0.8 eV with a full width at half maximum (FWHM) of 0.5—0.7 eV. The position and shape of the peak cannot be described as due to photoionization of trapped carriers; rather, a resonant transition seems to be involved. A transition between two bound levels of a localized state is improbable because in order for such a resonance to be observed in induced absorption, both initial and final levels must lie in the same half of the pseudogap. Thus the maximum transition energy is $E_g/2\sim 0.5-0.65$ eV, which is lower than the peaks found in the PA spectra.

Another resonant optical excitation is possible in systems where the electronic states are localized and strongly coupled to the lattice. In a photon-assisted hopping or optical charge transfer (OCT) transition, absorption of a photon is associated with motion of an electron in real space between two neighboring localized states. The photon energy appears as static distortion energy immediately after the transition, before the lattice has time to readjust to the new electron coordinates. This strain energy is partially or completely dissipated to the lattice vibrations during subsequent relaxation to a new equilibrium configuration. Using the Franck-Condon principle it is simple to show[30] that the thermal activation energy W_H for hopping between the two sites, the binding energy W_p of an electron at the site, and the OCT energy $\hbar\omega$ are related by

$$\hbar\omega = 2W_p \geq 2W_H \ ,$$

with equality on the right-hand side when there is no overlap between electronic wave functions on adjacent sites. The shape of the optical absorption band is roughly Gaussian with a width of $8(W_P\hbar\omega_0)^{1/2}$ at low tempertaures, where $\hbar\omega_0$ is the

energy of the lattice vibration to which the state is coupled.

The position and shape of the PA band in *a*-Ge:H can be well described by such a photon-assisted hopping transition if the binding energy of the localized state which captures the photocarriers is 0.35—0.40 eV. In Ref. 7, the normalized theoretical and experimental PA spectra were shown to be in close agreement when a value of 0.035 eV was used for the phonon energy $\hbar\omega_0$, based on the observed TO peak seen in vibrational spectroscopy.[31] This model also accounts for the observed independence of the PA linewidth on temperature [Fig. 7(a)] in our experimental range ($kT << \hbar\omega_0$).

When all the electronic states of a solid are localized by lattice distortion (small polaron formation), then the dc transport of carriers is also by hopping between localized states and the dc drift mobility should be correlated with the OCT absorption band.[30,32] However, such a comparison is meaningful only when it is known that dc charge transport and optical absorption are due to the *same* set of carriers. Results of recent dark dc transport measurements in *a*-Ge:H were interpreted as an indication that electrons in *a*-Ge:H form small polarons with W_H in the range 0.15—0.20 eV,[33] hence, a binding energy $W_p \gtrsim 0.3-0.4$ eV. While this is consistent with the OCT energy deduced from the PA peak, there is not sufficient data to conclude that the same carriers are responsible for dark dc transport and PA in this material. A study of the correlation between photoconductivity and PA may help to answer this question.

If small polarons are not formed in *a*-Ge:H, optical charge transfer can still occur at defect-related states. In fact, most experimental observations of the OCT absorption band correspond to the hopping of "bound polarons" between nearly equivalent sites associated with a lattice structural defect.[32,34] In this case the absorption will have no necessary relation to dc transport. In systems where only defect-bound small polarons are formed, an optical absorption band is observed but the dc transport properties do not show the characteristics of polaron hopping motion.

States in the gap of *a*-Ge:H have not been studied in as much detail as those in *a*-Si:H. Hence, if the PA in *a*-Ge:H is due to bound polarons it is difficult to make any definite statement about the nature of the defect state responsible for OCT. In order to exhibit this absorption band, the carrier must be able to occupy several (≥ 2) positions of nearly equivalent energy, and must be coupled to a similar lattice mode at each such site. For example, hopping may occur between the equivalent states of a vacancy complex or internal microvoid surface coupled to a distortion of the shape of the void. Alternatively, charge transfer between adjacent dangling bonds (dimer) might occur with an associated asymmetric stretch of the bonds between the Ge atoms in the dimer and those attached to the surrounding lattice.

In a defect OCT model, the broadening of the PA band in amorphous Si_xGe_{1-x} in going from $x=0$ to $x=0.6$ can be partially accounted for by an increasing average TO phonon energy $\hbar\omega_0$, which enters the expression for the FWHM of the polaron band as $(\hbar\omega_0)^{1/2}$. Broadening is also expected due to the increasing compositional disorder as Si is alloyed with Ge, as the site energies of defects associated with Si and Ge are expected to differ; in the more mixed alloys a larger proportion of defects involving nearby Si and Ge atoms is expected to occur.

When the alloy composition in *a*-Si_xGe_{1-x} becomes silicon-rich ($x \geq 0.6$), the PA spectra change from bound polaronlike symmetric bands to the asymmetric shape characteristic of trapped-hole photionization as discussed in Sec. V A. There are several reasons why this may occur. First, the electron-lattice interaction may be weaker in *a*-Si than in *a*-Ge. This is plausible since in these nonpolar materials the deformation potential interaction is correlated with the core polarizability which is greater in Ge. Also, the bulk modulus in Ge is about 30% lower than in Si, so distortions may not cost as much elastic energy. The special defect structure required for OCT (with two or more equivalent sites) may be more readily formed in *a*-Ge than in *a*-Si. It is well established that the overall density of states in the gap in glow-discharge deposited *a*-Ge:H is around ten times higher than in *a*-Si:H,[35] hence, structures like the dangling bond dimer may have a higher probability of occuring in Ge.

Another consequence of the higher density of gap states in *a*-Ge is that the trap quasi-Fermi-levels will lie closer to mid-gap in this material at a given excitation level. Since the occupied traps are farther from the band edges, the matrix elements for photoionization transitions will be smaller than they are for holes trapped at E_{tp} in *a*-Si. This may provide an explanation for the absence of trapped-hole photoionization in *a*-Ge and Ge-rich alloys.

Van Dong *et al.*[36] reported the composition

dependence of photoconductivity in sputtered a-Si_xGe_{1-x}:H. They also find a critical composition near $x=0.7$ where recombination kinetics change abruptly. The occurrence of a high density of localized states with enhanced electron-phonon coupling, which we have proposed to explain PA spectra in Ge-rich alloys, could also cause a discontinuous change in the recombination mechanisms controlling photoconductivity.

The PA spectrum of a-GaAs:H [Fig. 4(c)] shows a relatively sharp peak at 1.1 eV and well-resolved shoulder at 0.8 eV which may represent a superposition of two symmetric bands like those in a-Ge. If so, it is suggestive of two OCT absorption bands due to either (1) bound polarons at two types of defects with different W_p, (2) a defect-bound polaron and a free small polaron, or (3) free polarons formed by photogenerated carriers of both signs. The formation of free polarons in a-GaAs is perhaps made more likely by the electron-phonon interaction with the polar modes of the lattice. However, comparatively little information on electronic states in amorphous III-V materials is currently available and speculation about the origin of PA is premature.

Whatever the nature of the localized states reponsible for PA, they must be occupied when the sample is illuminated and empty in the dark. Thus the free carriers generated by light must either rapidly form small polarons or become trapped at defect-related gap states. As noted previously, additional evidence for the occupation of localized states in tetrahedral amorphous semiconductors under illumination comes from observations of photoinduced electron spin resonance (ESR) or photospin (PS) in a-Si:H and a-Ge:H.[4,5] A logical direction for future work is to correlate the PA spectrum and kinetics with those of PS, which can give additional information on the spin, charge, and local structural environment of the defects. Such an approach has been fruitful in elucidating the nature of defect states in crystalline semiconductors and insulators. It has also been suggested[37] that the same states responsible for PS in a-Si:H may take part in photoluminescence transitions, providing a third experimental probe of these states.

C. Steady-state recombination kinetics

The PA intensity, integrated over the entire band, is proportional to the density N of induced absorbing centers. In the steady state this density is governed by the rates of generation and recombination of these excitations and the experimental results can be explained by a simple model for these processes. Optical excitation generates a density N_f of free electrons and holes at a rate G; the carriers responsible for PA (presumably holes) are then rapidly trapped in the absorbing states in a time τ_t. The traps are deep so that thermal reemission into the valence band is neglected. Since the PA signal increases approximately as the square root of the pump intensity, recombination is bimolecular. Hence the appropriate rate equations for the density of free carriers and absorbing centers are

$$\frac{dN_f}{dt}=G-\frac{N_f}{\tau_t}\,, \tag{25}$$

$$\frac{dN}{dt}=\frac{N_f}{\tau_t}-bN^2\,, \tag{26}$$

where b is the bimolecular rate coefficient. The steady-state solutions are simply $N_f=G\tau_t$ and $N=(G/b)^{1/2}$.

The rate of a bimolecular reaction can be either diffusion limited or reaction limited, where, in this case, the relevant rates are that of diffusion of electrons towards trapped holes and exciton recombination, respectively. By exciton is meant the state which results after the fully thermalized electron and hole have diffused closely enough to one another that their (localized) wave functions overlap and recombination is more probable than further diffusion together. The slower of the two processes determines the rate. For a-Si:H and related amorphous semiconductors the diffusion coefficients of carriers are comparable to those of ions in liquid solution, so the diffusion times are very long. The diffusion-limited lifetime is $(bN)^{-1}$ and its value at low temperature can be calculated using the data of Fig. 10 and estimating the carrier density (using an absorption cross secton of 10^{-16} cm^2) to be $N\simeq 10^{16}$ cm^{-3}. We find roughly $(bN)^{-1}\simeq 4\times 10^{-6}$ sec. Exciton recombination is presumably nonradiative and governed by multiphonon emission. The lifetime should be much shorter than 4×10^{-6} sec unless there is a large energy barrier to multiphonon emission.[38] We assume that this is not the case and consider the recombination to be diffusion limited under our experimental conditions.

In low-mobility materials diffusion-limited recombinaton of oppositely charged species has

been treated by Langevin.[39] In this theory, the rate coefficient is

$$b=\frac{e}{\epsilon}(\mu_n+\mu_p) \tag{27}$$

where μ_n and μ_p are the drift mobilities of electrons and holes in their mutual Coulomb field. In a-Si:H $\mu_p << \mu_n$ and can be neglected in Eq. (27). Thus the bimolecular coefficient is directly proportional to the electron drift mobility; using (27) the data of Fig. 10 can be converted to give μ_n as a function of temperature. At room temperature μ_n is in the range 7×10^{-4}–4×10^{-3} cm^2/V sec, and at 80 K 4×10^{-6} to 10^{-5} cm^2/V sec. Literature values[21] of the electron drift mobility in a-Si:H derived from measurements of carrier drift in an applied field over macroscopic distances are not directly comparable due to the effects of anomalous dispersion.[9,40] Results of time of flight measurements are usually one or more orders of magnitude larger than our data; however, at this point no PA and drift mobility data on the same material are available.

In Fig. 11 the data are plotted as ln$b$ vs temperature for undoped and doped a-Si:H samples. The straight lines which result indicate that the drift mobility figuring in Eq. (27) has the unusual temperature dependence $\mu_n \propto \exp(T/T_1)$ with $T_1=31$, 67, and 106 K in undoped, B-, and P-doped a-Si:H, respectively.

The interpretation of the steady state time-averaged drift mobility μ_n is complicated by the fact that the nonequilibrium electrons are distributed in an unknown way over a continuous density of (localized and extended) states:

$$\mu_n(T)=\int_{E_F}^{\infty} f^*(E,T)g(E)\mu(E,T)dE \ , \tag{28}$$

where f^* is the occupation probability under steady-state photoexcitation, $g(E)$ is the density of states, and $\mu(E,T)$ is a suitably defined differential mobility characteristic of states at energy E. For $E>E_c$ (where E_c is the conduction-band mobility edge), $\mu(E,T)$ is expected to have a weak, scattering-limited dependence on T. Below E_c the differential mobility is much smaller but increases strongly with increasing temperature.

The strong increase of $\mu_n(T)$ with T cannot be explained by transport in extended states only. We will discuss a simple model which gives the observed temperature dependence of μ on T. We assume that $\mu(E,T)\simeq 0$ for $E<E_c$ and $\mu(E,T)=\mu_f$ for $E>E_c$. This is equivalent to the model of "trap limited" mobility used in the theory of photoconductivity in crystalline semiconductors and insulators[24] where the temperature dependence is due to the rate of thermal emission of trapped electrons from the localized states into states above E_c. Since this model depends only on the mobility μ_f, a trapping rate τ_n, and the energy distribution of traps below the band edge, the results can be taken over with only minor modifications to the case of amorphous semiconductors when the above assumption about $\mu(E,T)$ is made.

The localized-state distribution below the conduction-band mobility edge E_c is modeled by the function

$$g_T(E)=A\exp[-(E_c-E)/kT_0] \ , \tag{29}$$

i.e., the states are exponentially distributed below E_c with a characteristic width $kT_0>kT$. From the assumption about $\mu(E,T)$ and Eq. (28) we obtain for the drift mobility

$$\mu_n=\mu_f(n_f/n) \ , \tag{30}$$

where n_f is the density of electrons in states above E_c and n is the total excess electron density under steady-state photoexcitation. The equilibrium dark carrier density n_0 is negligible in undoped a-Si:H. From Eq. (27) the bimolecular rate coefficient b is related to μ_n by

$$b=\frac{e}{\epsilon}\mu_n=\frac{e}{\epsilon}\mu_f(n_f/n) \ . \tag{31}$$

Since excess electrons disappear by recombining with trapped holes, the total steady-state electron density is $n=(G/b)^{1/2}$, where G and b are the same parameters governing hole generation and recombination in Eqs. (25) and (26) above. Substituting into Eq. (31) yields

$$b=\left[\frac{e}{\epsilon}\mu_f\right]^2 n_f^2/G \ . \tag{32}$$

The free-carrier density n_f is determined by trapping into states near the free-electron quasi-Fermi-level F_n:

$$n_f=G\tau_n \ , \tag{33}$$

where the trapping rate τ_n is given by the product of the electron thermal velocity v, trapping cross section σ_T, and the density of traps near the quasi-Fermi-level F_n:

$$\tau_n^{-1}=v\sigma_T\{kT_0A\exp[-(E_c-F_n)/kT_0]\} \ . \tag{34}$$

The quasi-Fermi-level for electrons is determined by the definition

$$n_f = N_c \exp[-(E_c - F_n)/kT] , \quad (35)$$

where N_c is the effective density of extended states in the conduction band. Combining Eqs. (33)–(35), we obtain

$$\frac{n_f}{N_c} = \left[\frac{G}{v\sigma_T k T_0 A N_c} \right]^{T_0/(T+T_0)} , \quad (36)$$

which when substituted back into (32) gives

$$b = \beta \exp[-2T_0 \ln C/(T_0+T)] , \quad (37)$$

where

$$\beta = (e\mu_f/\epsilon)^2, \quad C = v\sigma_t k T_0 A N_c/G >> 1 . \quad (38)$$

For $T << T_0$, Eq. (37) reduces to

$$b \simeq e^{T/T_1} , \quad (39)$$

where

$$T_1 = T_0/2\ln C . \quad (40)$$

A good fit with the data in Fig. 11 is obtained by choosing $T_1 = 31$, 67, and 106 K for a-Si:H, a-Si:(B, H) and a-Si:(P, H), respectively. Assuming a reasonable value of $C \simeq 10^8$, the widths of the trap distribution kT_0 are found to be 0.09, 0.18, and 0.33 eV for the three samples. Note that the width of the electron-trap distribution near the quasi-Fermi level in undoped a-Si:H is nearly equal to that of the hole traps near E_{tp} as found in Sec. V A.

VI. SUMMARY AND CONCLUSIONS

A photoinduced optical absorption below the band gap has been observed by modulation spectroscopy in amorphous semiconducting thin films of various compositions, all belonging to the class of hydrogenated tetrahedrally bonded materials. Under continuous illumination the samples have PA spectra which fall into two groups. In a-Si:H and Si-C alloys with optical energy gaps from 1.4 to 2.0 eV, the absorption line shape has the form expected for transitions between a discrete level in the gap and a bandlike continuum. We tentatively identify the gap state as a donorlike defect lying from 0.3 to 0.6 eV above the top of the valence band and ascribe the PA to transitions of excess holes trapped there. In a-Ge:H and Si-Ge alloys with $E_G < 1.4$ eV, the PA spectra consist of single, symmetric bands characteristic of a resonant transition. The mechanism here is optical charge transfer (OCT) or photon-assisted hopping of excess carriers between neighboring sites of a defect with strong electron-lattice interaction. The binding energy associated with lattice distortion at an occupied site is 0.35–0.4 eV.

In the a-Si_xGe_{1-x}:H alloy system the change of the PA line shape from the asymmetric (photoionization) to the symmetric (OCT) form occurs discontinuously at a composition around $x = 0.6$. This can be attributed either to an increasing electron-lattice coupling as x decreases or to the presence of special defect structures at which OCT can occur in the Ge-rich alloys.

Photoinduced absorption below the band gap also exists in another class of amorphous semiconductors, the chalcogenide glasses and amorphous arsenic. The main phenomenological differences are that the inducing and decay rates in these glasses are much slower (at a given temperature) and their PA spectra always show the asymmetric form with a low-energy threshold at about half the band gap. A commonly accepted interpretation proposes[13,40] that PA in these materials is a manifestation of native defects, such as valence alternation pairs, which (by virtue of strong electron-lattice coupling) have the special property of negative effective electron-electron correlation energy. Induced absorption is caused by photoionization of excess carriers trapped by these defects. We have made no attempt at a detailed comparison of PA in the tetrahedral and chalcogenide semiconductors or at comparing our data with various recent models for defects in a-Si:H because the PA spectra do not contain information on the relationship between defect occupancy, spin and charge. The charged-defect model for chalcogenides results from a simultaneous interpretation of transport, ESR, and luminescence data. Since these properties are very sensitive to preparation conditions in the tetrahedral materials, comparative measurements must be made on the same samples. Indeed, even in the chalcogenides recent evidence suggests that the totality of experimental data cannot be explained if it is assumed that only one class of defect is important.

From the time decay of PA (Ref. 9) and the steady-state response to pump intensity and temperature, information about the recombination dynamics was also obtained. These measurements

were performed mainly in doped and undoped *a*-Si:H samples and the spectrally integrated PA intensity was taken as a measure of the total density of absorbing centers. This amounts to an assumption that essentially all the oscillator strength of photoexcited carriers is included with the PA band extending from about 0.3 to 1.6 eV. Under our experimental conditions the recombination process was found to be bimolecular and diffusion limited; that is, holes and electrons recombine directly with the slow diffusion of an electron into the capture sphere of a trapped hole being the rate-determining step. Two interesting properties of electron mobility μ_n are exhibited in these measuremens. First, in a time range from 5×10^{-7} to 10^{-3} sec following pulsed excitation, the recombination rate indicates that μ_n is a decreasing function of time.[9] This is the expected result of the anomalous dispersion of the drift velocities of nonequilibrium carriers commonly observed in amorphous materials and treated theoretically by Scher and Montroll.[41] Ngai and Liu[42] show that the formulas proposed for describing our experimental results follow from their approach to the dispersive transport.

Using the PA technique the time-averaged electron drift mobility was measured over a larger temperature range than that accessible to electrical measurements. The unusual temperature dependence $\mu_n \sim \exp(T/T_1)$ was found, with $T_1 = 31$, 67, and 106 K in B-doped, P-doped, and undoped *a*-Si:H samples, respectively. A drift mobility having this form was explained by assuming that electrons are repeatedly trapped and released from an exponential distribution of localized states below the conduction-band mobility edge.

Induced absorption spectroscopy has been shown to be a useful probe of the tetrahedral amorphous semiconductors in a state of high photoexcitation, providing new information about the poorly understood fundamental process of carrier trapping, diffusion, and recombination. Further work correlating this and related photoeffects is necessary to achieve a more complete knowledge of the structure and electronic characteristics of the defects which influence these processes in real samples.

ACKNOWLEDGMENTS

We are grateful to Professor W. Paul and Dr. M. Brodsky, Dr. C. R. Guarnieri, Dr. J. C. Knights, Dr. M. A. Paesler, Dr. R. A. Street, and Dr. H. Wieder for generously providing samples for this study. We wish to acknowledge stimulating discussions with Professor M. Kastner and Dr. D. E. Ackley, Dr. E. C. Freeman, and Dr. Z. Vardeny as well as the technical assistance of Mr. T. R. Kirst. This work was supported in part by National Science Foundation Grants Nos. DMR76-17443 A01 and DMR79-09819, and the NSF Materials Research Laboratory at Brown University.

---

*Present address: Bell Laboratories, Murray Hill, New Jersey 07974.

[1]W. Spear and P. LeComber, Philos. Mag. 33, 935 (1976); D. Anderson and W. E. Spear, *ibid.* 36, 695 (1977).

[2]R. S. Crandall, Phys. Rev. Lett. 44, 749 (1980); J. Pankove, F. Pollack, and C. Schnabolk, J. Non-Cryst. Solids 35&36, 459 (1980).

[3]D. Engemann and R. Fischer, Phys. Status Solidi B 79, 195 (1977); T. S. Nashashibi, I. G. Austin, and T. M. Searle, Philos. Mag. 35, 831 (1972); C. Tsang and R. Street, *ibid.* 37, 601 (1979); J. Pankove and D. Carlson, Appl. Phys. Lett. 31, 450 (1977).

[4]J. C. Knights, D. Biegelson, and I. Solomon, Solid State Commun. 22, 133 (1977).

[5]J. R. Pawlik and W. Paul, in *Proceedings of the 7th International Conference on Amorphous and Liquid Semiconductors, Edinburgh, 1977,* edited by W. Spear (Center for Industrial Liasion, University of Edinburgh, 1977), p. 437.

[6]R. A. Street, Phys. Rev. B 17, 3984, (1978); D. Bishop, U. Strom, and P. Taylor, Phys. Rev. Lett. 34, 1346 (1975).

[7]P. O'Connor and J. Tauc, Phys. Rev. Lett. 43, 311 (1979).

[8]P. O'Connor and J. Tauc, J. Non-Cryst. Solids 35&36, 699 (1980).

[9]Z. Vardeny, P. O'Connor, S. Ray, and J. Tauc, Phys. Rev. Lett. 44, 1267 (1980).

[10]P. O'Connor and J. Tauc, Solid State Commun. 36, 947 (1980).

[11]P. O'Connor, thesis, Brown University, 1980 (unpublished).

[12]T. Staflin and L. Huldt, Arc. Phys. 20, 526 (1961).

[13]N. Mott, E. A. Davis, and R. Street, Philos. Mag. 32, 961 (1975); M. Kastner, D. Adler, and H. Fritzsche, Phys. Rev. Lett. 37, 1504 (1976); M. Kastner and H. Fritzsche, Philos. Mag. B 37, 199 (1978).

[14]V. K. Subashiev, Surf. Sci. 37, 947 (1973).
[15]J. Shive, J. Appl. Phys. 18, 398 (1947).
[16]E. C. Freeman and W. Paul, Phys. Rev. B 20, 716 (1979).
[17]M. Brodsky and P. Leary, J. Non-Cryst. Solids 35&36, 487 (1980).
[18]A. Onton, H. Wieder, J. Chevallier, and C. R. Guarnieri, in Ref. 5, p. 357.
[19]A. Gheorghieu and M. L. Theye, J. Non-Cryst. Solids 35&36, 397 (1980).
[20]T. Tiedje and A. Rose, Solid State Commun. 37, 49 (1981).
[21]A. Moore, Appl. Phys. Lett. 31, 762 (1977); D. Allen, P. LeComber, and W. Spear, in Ref. 18, p. 323.
[22]L. Vieux-Rochaz and A. Chenevas-Paule, J. Non-Cryst. Solids 35&36, 737 (1980).
[23]P. E. Vanier and R. W. Griffith, Bull. Am. Phys. Soc. 25, 330 (1980); P. D. Persans and H. Fritzsche, in *Tetrahedrally Bonded Amorphous Semiconductors,* edited by R. A. Street, V. K. Biegelson, and J. C. Knight (AIP, New York, 1981), p. 238.
[24]A. Rose, *Concepts in Photoconductivity and Allied Problems* (Interscience, New York, 1963).
[25]G. Moddel, D. A. Anderson, and W. Paul, Phys. Rev. B 22, 1918 (1980).
[26]E. Hauser, J. Tauc, and J. J. Hauser, Solid State Commun. 32, 285 (1979).
[27]M. Olivier, J. C. Peuzin, and A. Chenevas-Paule, J. Non-Cryst. Solids 35&36, 693 (1980).
[28]J. Stuke, in Ref. 5, p. 406; U. Voget-Grote, W. Kummerle, R. Fischer, and J. Stuke, Philos. Mag. 41, 141 (1980).
[29]D. K. Biegelsen and R. A. Street, Phys. Rev. Lett. 44, 803 (1980).
[30]I. G. Austin and N. Mott, Adv. Phys. 18, 41 (1969); D. Emin, *ibid.* 24, 305 (1975).
[31]M. Brodsky and A. Lurio, Phys. Rev. B 9, 1646 (1979).
[32]V. N. Bogomolov, E. K. Kudinov, D. N. Mirlin, and Y. A. Firsov, Fiz. Tverd. Tela (Leningrad) 9, 2077 (1967) [Sov. Phys.—Solid State 9, 1630 (1968)]; V. N. Bogomolov and D. N. Mirlin, Phys. Status Solidi B 27, 443 (1968).
[33]A. J. Lewis, Phys. Rev. B 13, 2565 (1976).
[34]O. Schirmer, Solid State Commun. 18, 1349 (1976); M. Monakata, Solid State Electron. 1, 159 (1960); T. N. Kennedy and J. D. MacKenzie, J. Phys. Chem. Glass 8, 169 (1967).
[35]D. I. Jones, W. Spear, and P. G. LeComber, J. Non-Cryst. Solids 20, 259 (1976).
[36]N. Van Dong, T. H. Danh, and J. Y. Leny, J. Appl. Phys. 52, 338 (1981).
[37]D. Biegelson, R. Street, C. C. Tsai, and J. Knights, J. Non-Cryst. Solids 35&36, 285 (1980).
[38]N. Mott and A. M. Stoneham, J. Phys. C 10, 3391 (1977).
[39]P. Langevin, Ann. Chem. Phys. 28, 289, 433 (1903).
[40]G. S. Bishop, U. Strom, and P. C. Taylor, Phys. Rev. Lett. 34, 1346 (1975); Phys. Rev. B 15, 2278 (1977); P. C. Taylor, U. Strom, and S. G. Bishop, Philos. Mag. B 37, 241 (1978).
[41]H. Scher and E. Montroll, Phys. Rev. B 12, 2445 (1975).
[42]K. L Ngai and F. Liu, Phys. Rev. B 24, 1049 (1981).